Fully-Reconfigurable Non-Reciprocal Bandpass Filters

Dakotah Simpson^{#1} and Dimitra Psychogiou^{#2}

*Dept. of Electrical, Computer, and Energy Eng., University of Colorado, Boulder, CO, USA ¹Dakotah.Simpson@colorado.edu, ²Dimitra.Psychogiou@colorado.edu

Abstract—This paper reports on the RF design of quasi-elliptic non-reciprocal bandpass filters (BPFs) with fully-reconfigurable transfer function. It is demonstrated that by modulating the resonant frequency of its constituent resonators, the RF signal propagation is only enabled in one direction-e.g., from port 1-to-2-whereas it is sufficiently suppressed in the reverse one. Furthermore, by varying the resonant frequency of the BPF's resonators, the transfer function in the forward direction can be tuned in terms of frequency and bandwidth (BW) and can be intrinsically switched-off. For practical demonstration purposes, a lumped-element prototype centered at 300 MHz was designed manufactured and measured. It demonstrated a 1.15:1 center frequency tuning and a 2.77:1 BW tuning range while maintaining a non-reciprocal behavior. For all tuning states, the minimum inband insertion loss in the forward direction was measured between 1.7 and 4.3 dB, whereas the isolation in the reverse direction was measured up to 30.9 dB.

Keywords—bandpass filter (BPF), lumped-element filter, nonreciprocal filter, spatiotemporal modulation, tunable filter.

I. INTRODUCTION

Non-reciprocal microwave components—i.e., isolators and circulators—are critical in protecting sensitive RF devices from reflected high-power signals and are fundamental elements of full-duplex radios due to their primer role in separating their transmit and receive channels. Despite the necessity of these components in many radar and communication systems, their practical development has been hindered by the need for bulky magnetically-biased ferrite-based resonators.

Recent research efforts are focusing on reducing the size of the RF front-ends of these systems either by developing magnet-less non-reciprocal devices [1]-[8] or by incorporating RF co-designed components with collocated signal processing capabilities (e.g., co-designed filters/power dividers [9] or filters/matching networks [10]). Early magnet-less concepts exploited the inherent non-reciprocal properties of transistors or used operational-amplifier-based stages [1], [2]. However, they suffered from poor noise performance and strong nonlinearities. RF circulators using self-biased materials have also been presented [11]. However, these concepts, exhibit high insertion loss (IL) (up to 8 dB) and are not compatible with advanced CMOS or MMIC integration platforms.

In yet another configuration, non-reciprocal components are created by breaking the time-reversal symmetry in two-/threeport networks. For example, in [3] linear periodically timevariant N-path filters break reciprocity through staggered commutation [3]. Spatiotemporal modulation (STM) has also been proposed as an effective mechanism in optical devices and is nowadays applied to the realization of non-reciprocal microwave circulators/isolators, [4], [5]. In particular, [5] demonstrates the potential to achieve non-reciprocity in a

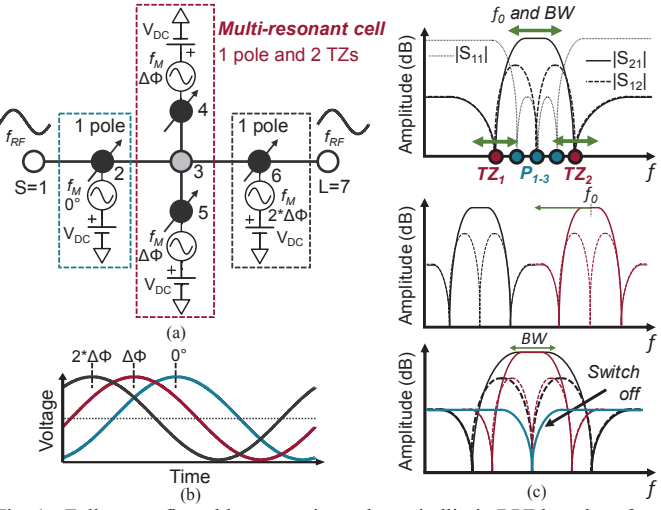


Fig. 1. Fully reconfigurable non-reciprocal quasi-elliptic BPF based on four spatiotemporally-modulated resonators. (a) Coupling-routing diagram. White circles: source and load; grey circle: non-resonating node; black circles: frequency tunable, f_M -modulated resonating nodes ($f_M \ll f_{RF}$); black lines: impedance inverters. (b) Conceptual illustration of the AC modulation signals applied to the varactor-based resonators. (c) Conceptual power transmission ($|S_{21}|$), reflection ($|S_{11}|$), and isolation ($|S_{12}|$) responses of the fullyreconfigurable non-reciprocal BPF including center frequency tuning, BW tuning and intrinsic switching off.

circulator by introducing a biasing scheme that imparts angular momentum into the resonators of inter-connected resonant rings. RF co-designed methods of isolators/filters are also being investigated [6]-[8] for size reduction purposes. However, they are mostly focused on the realization of static transfer function in the direction of propagation.

To further reduce the RF front-end size, this paper reports for the first time on a magnet-less non-reciprocal quasi-elliptic BPF that is fully reconfigurable in terms of multiple transfer function characteristics including center frequency, bandwidth (BW), and intrinsic switching off. Non-reciprocity is achieved through the STM of the BPF's resonators with progressively phase-shifted AC signals. The rest of this paper is organized as follows. In Section II, the operational and design principles of the non-reciprocal BPF are demonstrated. The experimental validation of the concept is reported in Section III. Lastly, the contributions of this work are summarized in Section IV.

II. THEORETICAL FOUNDATIONS

A. Non-Reciprocal Tuning Concept

The details of the non-reciprocal quasi-elliptic BPF with multiple levels of RF tuning are shown in Fig. 1 in terms of coupling-routing diagram and conceptual power transmission $(|S_{21}|)$, isolation $(|S_{12}|)$, and reflection $(|S_{11}|)$. The filter is

comprised of four frequency-tunable resonators—their resonant frequencies are determined by the DC and AC biasing imparted on their varactor-based capacitors—, one non-resonating node (NRN), and static impedance inverters. In the forward direction, the BPF exhibits a quasi-elliptic transfer function [12]. Specifically, resonating nodes 2 and 6 introduce two frequency-reconfigurable poles (P₁, P₂ in Fig. 1(a)). Resonating nodes 4 and 5, along with the NRN, shape the multi-resonant cell, which introduces two tunable transmission zeroes (TZs) and one additional pole (P₃). The two TZs (T_{Z1}, T_{Z2}) are located at the resonant frequencies of nodes 4 and 5 and the pole is located at the frequency at which the two paths in the multi-resonant cell have equal magnitude and opposite sign admittances. As such, the conceptual transfer function in the forward direction (|S₂₁|) consists of three poles and two TZs.

Whereas DC biasing sets the nominal resonator capacitance, the time-dependent AC biasing determines the directionality of the RF signal propagation. By appropriately selecting the frequency, f_M , the amplitude, V_M , and the phase progression, $\Delta \Phi$, of the AC signals – Fig. 1(b) – non-reciprocity can be achieved in the overall BPF transfer function as shown in Fig. 1(c). By altering the DC biasing of each resonator, the overall transfer function can be tuned in terms of center frequency and BW and can be intrinsically switched-off. Specifically, frequency tuning is attained by simultaneously tuning the resonant frequencies of all resonators. Furthermore, the passband can be varied by controlling the location of the TZs through the tuning of the resonators in the multi-resonant cell. For example, to obtain a narrower BW, the two TZs are simultaneously brought closer to the passband center frequency. Lastly, intrinsic switching off can be achieved by setting all resonators at the same frequency. In all of the aforementioned tuning states, f_M needs to be altered for maximum isolation at f_{cen} .

B. Design and Operating Principles

Fig. 2 shows the circuit-equivalent of the non-reciprocal quasi-elliptic BPF along with the AC/DC biasing scheme that allows modulation of the resonators' capacitances. In this representation, the static impedance inverters between nodes 1-3, 6, and 7 have been implemented with their first-order highpass π -type circuit equivalent. The resulting shunt elements of the inverters at the location of resonating nodes 2 and 6 have been absorbed into the resonators. However, since node 3 is a NRN, a single inductor (L_N) is left as a residual from this transformation. Furthermore, resonating nodes 4 and 5 have

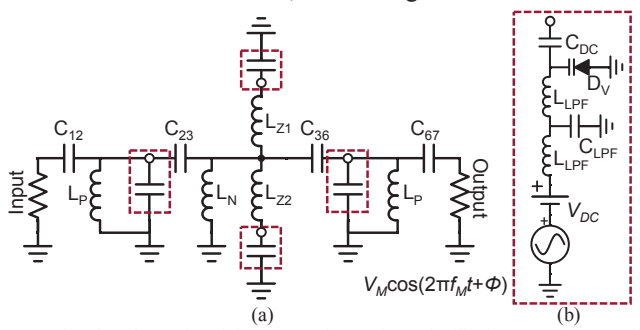


Fig. 2. Circuit-schematic of the non-reciprocal quasi-elliptic BPF. (a) Overall BPF architecture. (b) Detailed schematic of the DC biasing and AC modulation network for each of the resonators.

been combined with their connecting impedance inverters and are equivalently realized as series-type LC resonators to miniaturize and simplify the overall design. Fig. 2(b) shows the biasing scheme for every resonator capacitance. In particular, a varactor diode (D_V) is biased by both DC and AC signals through a lowpass filter (two inductors (L_{LPF}) and one capacitor (C_{LPF})). A DC blocking capacitor (C_{DC}) is added to block the DC signal from entering other resonators.

The non-reciprocal filter design is performed as follows. First, a reciprocal BPF is designed using conventional coupled-resonator techniques for the desired center frequency and BW without considering any AC modulation. This defines the correct DC biasing for the given varactor diodes and determines the component values in the schematic in Fig. 2. Afterwards, the AC modulation parameters, f_M , V_M , and $\Delta\Phi$ are obtained through optimization based on the desired in-band IL in the forward direction and the isolation in the reverse direction.

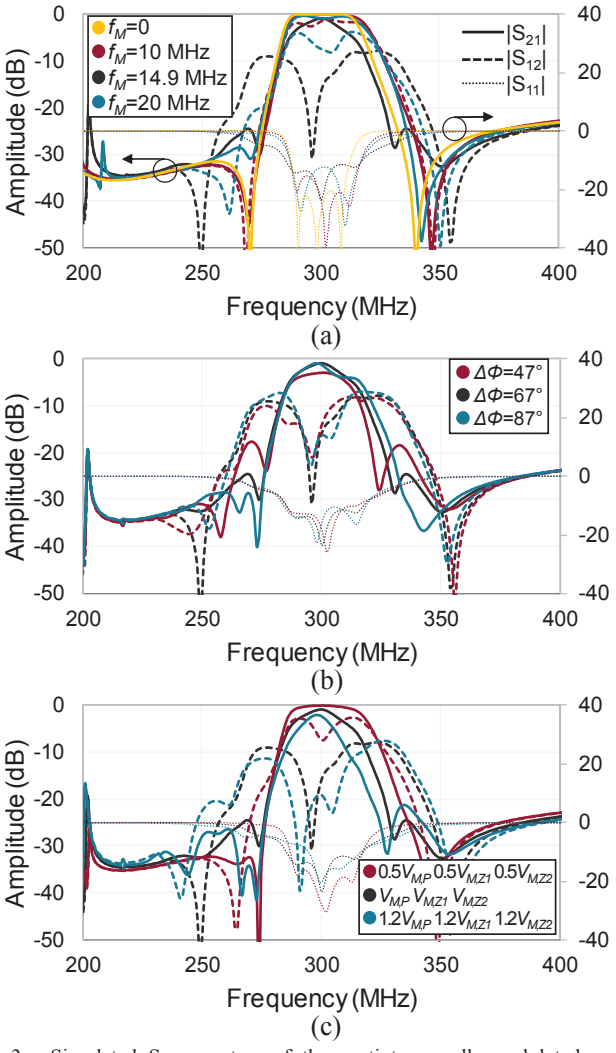


Fig. 3. Simulated S-parameters of the spatiotemporally-modulated non-reciprocal quasi-elliptic BPF as a function of the modulation parameters. (a) Variation of modulation frequency, f_M . (b) Variation of phase offsets, $\Delta\Phi$. (c) Variations of the amplitude of the modulation signal, V_M . The values used for the non-varied reference responses are f_M =14.9 MHz, $\Delta\Phi$ =67°, $V_{M,P}$ =420 m V_{PP} , $V_{M,Z1}$ =180 m V_{PP} , and $V_{M,Z2}$ =120 m V_{PP} . In these examples, C_{12} = C_{67} =4 pF, C_{23} = C_{36} =4.5 pF, L_P =20.3 nH, L_N =29.6 nH, L_Z =59.8 nH, L_Z =35.3 nH, C_{DC} =82 pF, L_{LPF} =310 nH, C_{LPF} =150 pF, and D_V is the Skyworks SMV1413.

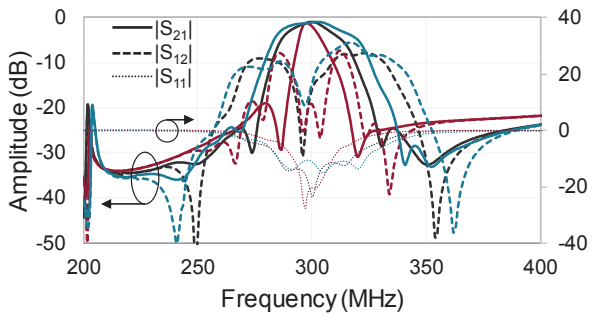


Fig. 4. Simulated S-parameters of the spatiotemporally-modulated nonreciprocal quasi-elliptic BPF as the BW is tuned.

To illustrate the aforementioned design steps, a BPF is designed for a center frequency of 300 MHz and a BW of 30 MHz (10%). Its simulated response without the presence of AC modulation is shown in Fig. 3(a) (yellow trace). Ideal lumpedelement components and commercially available varactors (loss omitted), Skyworks SMV1413 (capacitance range: 1.77-9.24 pF), were used. The BPF response in the presence of AC modulation is depicted in Fig. 3 for numerous variations of the AC signal. In particular, Fig. 3(a) shows how the BPF response changes with varying f_M as $\Delta \Phi$ and V_M are kept constant at the values shown in the caption of Fig. 3. As it can be seen, too low $(f_M=10 \text{ MHz})$ or too high $(f_M=20 \text{ MHz})$ of a modulation frequency results in low isolation levels in the reverse transmission. It is found that a modulation frequency of around 14.9 MHz gives low IL in the forward transmission and high isolation in the reverse transmission. As it can be observed, the optimum f_M is about half of the passband BW as also discussed in the BPF concept in [6].

In Fig. 3(b) the phase progression, $\Delta \Phi$, is altered and it is shown that this parameter affects not only the isolation in the reverse transmission but also the in-band IL and passband symmetry in the forward transmission. The highest isolation and most symmetric passband response is obtained when $\Delta \Phi =$ 67°. Lastly, Fig. 3(c) shows variations in the magnitude of the AC signals. As shown, too small of a magnitude results in low isolation whereas too large of a magnitude results in high inband IL. In Fig. 4, the BW of the filter is tuned by varying the location of the TZs relative to the center frequency of the passband. In this case, the modulation frequency needs to be proportionally readjusted as the BW is varied. Lastly, Fig. 5 shows the response of the BPF with varactor loss included and omitted. As shown, the SMV1413 varactors introduces □0.5 dB of loss and the rest of the remaining IL (\sim 1 dB) is a result of lost power to intermodulation products—i.e., never converted back to the RF signal—, as also shown in [4]-[6].

III. EXPERIMENTAL VALIDATION

To validate the proposed non-reciprocal quasi-elliptic tunable BPF concept, a lumped-element prototype was designed, manufactured, and measured. It was designed for a center frequency of 300 MHz and a BW (with AC modulation included) of 25 MHz (8.3%). The design was performed in ADS from Keysight while using the design in Section II. A photograph of the manufactured prototype is shown in Fig. 6. To provide both the DC and AC biasing, four clock-synced

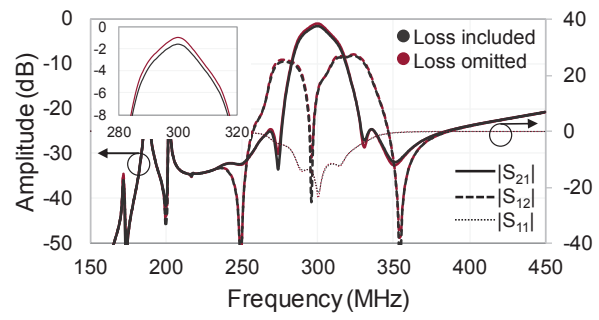
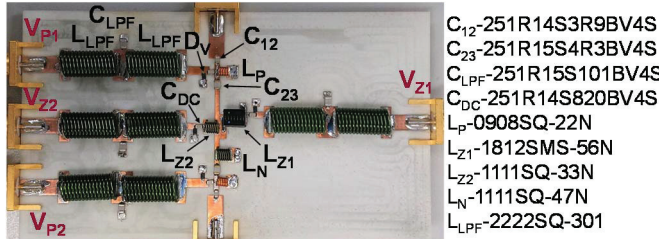


Fig. 5. Simulated S-parameters of the non-reciprocal quasi-elliptic BPF with and without loss in the varactor diodes. In these examples, $f_N=14.9$ MHz, $\Delta\Phi$ =67°, $V_{M,P}$ =420 m V_{PP} , $V_{M,ZI}$ =180 m V_{PP} , and $V_{M,Z2}$ =120 m V_{PP} .

arbitrary waveform generators (AWGs) are used. The RF transmission, isolation, and reflection responses were measured in terms of S-parameters using a Keysight N5224A PNA.

Fig. 7 demonstrates one RF measured response of the nonreciprocal BPF alongside with its corresponding EM simulated one, which appear to be in a good agreement, successfully validating the proposed non-reciprocal BPF concept. The measured center frequency and BW are 300.6 MHz and 25.8 MHz (8.6%), respectively. The minimum in-band IL of the forward transmission response ($|S_{21}|$) was measured to be 2.5 dB and the maximum isolation in the reverse direction ($|S_{12}|$) was measured to be 23.8 dB.

Fig. 8 characterizes the tuning capabilities of the prototype in terms of center frequency, BW, and intrinsic switching off. In particular, Fig. 8(a) shows that the center frequency of the transfer function can be tuned from 270 MHz to 310 MHz (1.15:1 tuning ratio) by simultaneously varying the DC biasing of all resonators. In Fig. 8(b), the BW tuning capabilities of the BPF are shown for a fixed center frequency passband. As it can be seen, its BW can be tuned from 15 MHz to 41.5 MHz (2.77:1). Though a finite number of responses is demonstrated, the filter can be continuously tuned in terms of frequency and BW. Throughout all the tuning responses, the minimum in-band IL in the forward transmission direction varies between 1.7-4.3 dB. Furthermore, the maximum isolation in the reverse direction is between 15.4-30.9 dB, and the in-band return loss is greater than 10 dB. It should be noted that each measurement state requires adjustments to the modulation parameters to obtain optimal non-reciprocity. For example, as the DC bias voltage of a resonator decreases, the AC magnitude must also be decreased to maintain a similar ratio of swing capacitance to nominal capacitance. Furthermore, as the BW of the forward transmission response varies, the frequency of modulation must be varied in the same fashion, e.g. as BW is decreased, f_M is also decreased such that $f_M \approx BW/2$. Lastly, Fig. 8(b) shows the intrinsic switching off (yellow trace) of both the forward and



C₂₃-251R15S4R3BV4S C_{LPF}-251R15S101BV4S C_{DC}-251R14S820BV4S L_p-0908SQ-22N L_{Z1}-1812SMS-56N L_{Z2}-1111SQ-33N L_N-1111SQ-47N

Fig. 6. Photograph of the non-reciprocal quasi-elliptic BPF prototype.

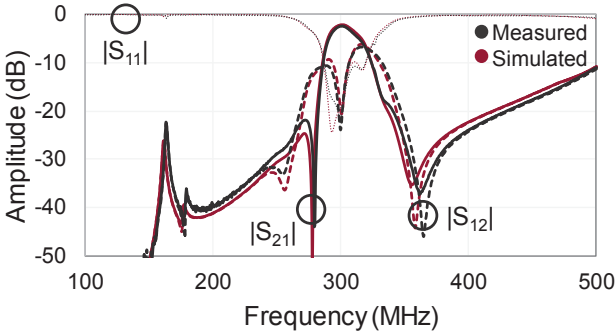


Fig. 7. Comparison of the RF-measured and EM-simulated S-parameters of one tuning state of the manufactured prototype in Fig. 6.

reverse transmission responses by turning off the modulation and setting their resonant frequencies equal to the same value. A comparison of the proposed filter with other non-reciprocal BPFs is provided in Table 1. As shown, this is the only non-reciprocal BPF in which multiple levels of tunability can be obtained. In addition, the obtained transfer function in the direction of propagation shows the highest selectivity/roll-off.

IV. CONCLUSION

Fully-reconfigurable non-reciprocal magnet-less BPFs are reported in this work for the first time. Non-reciprocity is achieved by spatiotemporally modulating its constituent resonators with progressively phase-shifted AC signals. This results in an imparted directionality within the BPF with high levels of isolation between the forward and reverse transmission paths. While the AC biasing of the resonators controls the directionality, DC biasing is used on the resonators' varactor diodes to the tune the overall filter response in terms

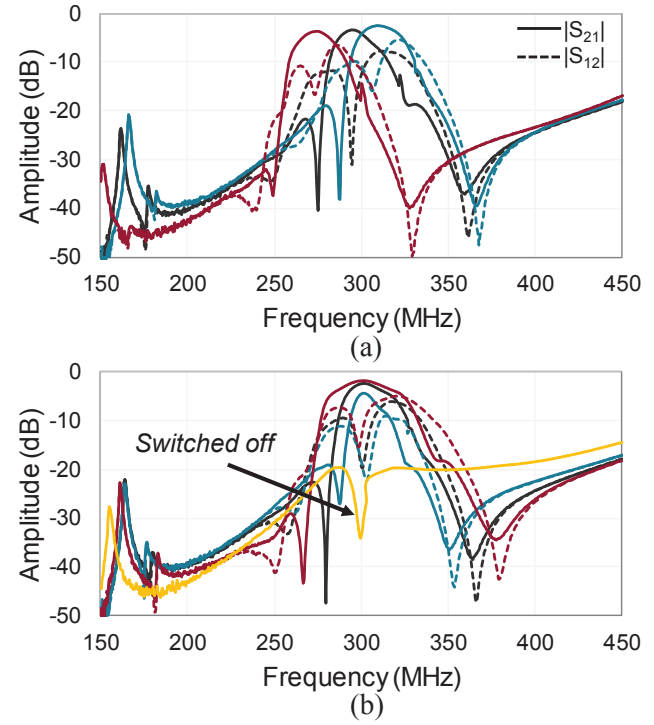


Fig. 8. RF-measured tuning capabilities of the manufactured prototype in Fig. 6 in terms of S-parameters. (a) Center frequency tuning. (b) BW tuning and intrinsic switch-off (yellow trace).

Table 1. Comparison of non-reciprocal BPFs. OFF – Intrinsic switching off, IS: maximum isolation

Ref	fcen (MHz)	BW (MHz)		Roll-off (dB/oct)		f _{cen} tuning	BW tuning	Off
[6]	187	33	1.5	90	23	No	No	No
[7]	1000	65	5.5	160	11.7	No	No	No
[8]	136- 163	27.5	3.7- 4.1	120	52.8	Yes (1.2:1)	No	No
This work	270- 310	15- 41.5	1.7- 4.3	360	30.9	Yes (1.15:1)	Yes (2.77:1)	Yes

of center frequency, BW, and intrinsic switching. For a proof-of-concept, a lumped-element prototype was designed and measured at a center frequency of 300 MHz. It exhibits isolation levels up to 30.9 dB, a 1. 15:1 center frequency tuning range, and a 2.77:1 BW tuning range while maintaining a non-reciprocal behaviour.

ACKNOWLEDGMENT

This work has been supported in part by the National Science Foundation under Grant ECCS-1731956 and ECCS-1941315.

REFERENCES

- S. W. Y. Mung and W. S. Chan, "Active three-way circulator using transistor feedback network," *IEEE Microw. Wireless Compon. Lett.*, vol. 27, no. 5, pp. 476-478, May 2017.
- [2] P. Chen and R. M. Narayanan, "Design of active circulators using high-speed operational amplifiers," *IEEE Microw. Wireless Compon. Lett.*, vol. 20, no. 10, pp. 575-577, Oct. 2010.
- [3] N. Reiskarimian and H. Krishnaswamy, "Fully-integrated non-magnetic non-reciprocal components based on linear periodically-time-varying circuits," 2017 IEEE 17th Topical Meeting Silicon Monolithic Integrated Circuits in RF Systems (SiRF), Phoenix, AZ, 2017, pp. 111-114.
- [4] A. Kord, D. L. Sounas, and A. Alù, "Differential magnetless circulator using modulated bandstop filters," 2017 IEEE MTT-S Intern. Microw. Symp. (IMS), Honolulu, HI, 2017, pp. 384-387.
- [5] N. A. Estep, D. L. Sounas, and A. Alù, "Magnetless microwave circulators based on spatiotemporally modulated rings of coupled resonators," *IEEE Trans. Microw. Theory Techn.*, vol. 64, no. 2, pp. 502-518, Feb. 2016.
- [6] X. Wu, X. Liu, M. D. Hickle, D. Peroulis, J. S. Gómez-Díaz, and A. Álvarez Melcón, "Isolating bandpass filters using time-modulated resonators," *IEEE Trans. Microw. Theory Techn.*, vol. 67, no. 6, pp. 2331-2345, June 2019.
- [7] X. Wu, M. Nafe, A. A. Melcón, J. Sebastián Gómez-Díaz and X. Liu, "A non-reciprocal microstrip bandpass filter based on spatio-temporal modulation," 2019 IEEE MTT-S Intern. Microw. Symp. (IMS), Boston, MA, USA, 2019, pp. 9-12.
- [8] D. Simpson and D. Psychogiou, "Magnet-less non-reciprocal bandpass filters with tunable center frequency", Proc. 49th European Microwave Conference (EuMC), 2019, Paris, France, 2019.
- [9] C. Zhu and J. Zhang, "Design of high-selectivity asymmetric three-way equal wideband filtering power divider," *IEEE Access*, vol. 7, pp. 55329-55335, 2019.
- [10] J. Jeong, P. Kim, P. Pech, Y. Jeong, and S. Lee, "Substrate-integrated waveguide impedance matching network with bandpass filtering," 2019 IEEE Radio Wireless Symposium, Orlando, FL, USA, 2019, pp. 1-3.
- [11] G. Hamoir, L. Piraux, and I. Huynen, "Control of microwave circulation using unbiased ferromagnetic nanowires arrays," *IEEE Trans. Magnetics*, vol. 49, no. 7, pp. 4261-4264, July 2013.
- [12] R. Gómez-García, J.-M. Munoz-Ferreras and D. Psychogiou, "Fully-reconfigurable bandpass filter with static couplings and intrinsic-switching capabilities", 2017 IEEE MTT-S International Microwave Symposium Digest (IMS), Honolulu, HI, USA, June 4-7 2017.